View metadata, citation and similar papers at core.ac.uk
brought to you by CORE
provided by NASA Technical Reports Server

THE UNIVERSITY OF NEW MEXICO

N71-25377
NASA CR-118330

Bureau of Engineering Research

Albuquerque

A STUDY OF METAL-INSULATOR-SEMICONDUCTOR MAGNETORESISTANCE, BULK, AND SURFACE PROPERTIES OF INDIUM ANTIMONIDE

by

T. W. Kim

W. W. Grannemann

Progress Report PR-97(71)NASA-028

March 1971

CASE FILE COPY

Prepared for National Aeronautics and Space Administration under Grant No. NGR32-004-002

A STUDY OF METAL-INSULATOR-SEMICONDUCTOR MAGNETORESISTANCE, BULK, AND SURFACE PROPERTIES OF INDIUM ANTIMONIDE

by

T. W. Kim

W. W. Grannemann

Progress Report PR-97(71)NASA-028

March 1971

Prepared for National Aeronautics
and Space Administration
under Grant No. NGR32-004-002

CONTENTS

		Page
1.0	Introduction	1
2.0	Theory and Expected Results from the Experiments	2
	2.1 Equations for the Magnetoresistance Devices	2
	2.2 Calculations of the Magnetoresistance of the MIS Devices	10
3.0	Electron Beam Source and Proposed Experimental Work	36
	3.1 Basic Principles	37
	3.2 Specifications	38
	3.3 Advantages	38
	3.4 Proposed Experimental Work	40
4.0	Conclusions	41
5.0	References	42

LIST OF ILLUSTRATIONS

Figure		Page
1	Dependence of electron mobility on impurity concentration for n-type InSb at room temperature (Reference 6)	10
2	Temperature vs. mobility, Hall coefficient and conductivity for InSb thin films (Reference 7)	11
3	Corbino disk magnetoresistance vs. magnetic induction B	14
4	Corbino disk magnetoresistance for two conduction bands vs. magnetic flux density (strong field)	16
5	Corbino disk magnetoresistance for two conduction bands vs. magnetic flux density (low field)	17
6	Magnetoresistance of two-layer corbino disks vs. magnetic flux density	19
7	Mutual conductances and drain-source resistance vs. drain-source voltage	22
8	MIS slab resistance vs. magnetic flux density when $\theta = 1.0$	26
9	MIS slab resistance vs. magnetic flux density when $\theta = 0.5$	27
10	MIS slab resistance vs. magnetic flux density when $\theta = 0.1$	28
11	MIS corbino disk drain-source resistance vs. drain-source voltage	30
12	Drain-source resistance vs. gate-source voltage as a function of θ	32
13	MIS corbino disk magnetoresistance vs. magnetic-flux density when $\theta = 1.0$	34
14	MIS corbino disk magnetoresistance vs. magnetic-flux density when $\theta = 0.1$	35
15	Electron beam source	39
16	Electron gun magnetic focusing system	39

A STUDY OF METAL-INSULATOR-SEMICONDUCTOR MAGNETORESISTANCE, BULK, AND SURFACE PROPERTIES OF INDIUM ANTIMONIDE

1.0 Introduction

This report presents a discussion of the metal-insulator-magnetoresistance, bulk, and surface properties of the indium antimonide compound semiconductor material.

The vacuum system modified by The University of New Mexico research team (Reference 1) has made the research of the compound semiconductor materials possible. Furthermore, the vacuum system is under modification to improve the capability for vacuum deposition of the compound materials. The electron beam source and its control system will be adapted to the vacuum system.

In order to obtain the best metal-insulator-semiconductor magnetoresistance devices, the maximum theoretical limits and expected experimental results should be known before fabrication and measurement. Calculations from the given data involve the corbino disk magnetoresistance MIS thin-film transistor, magnetoresistance of the MIS thin-film device, and MIS corbino disk magnetoresistance. The individual characteristic curves, i.e., magnetoresistance versus magnetic field, will be drawn to compare the theoretical results to the experimental ones.

2.0 Theory and Expected Results from the Experiments

2.1 Equations for the Magnetoresistance Devices

2.1.1 Corbino Disk

The expression for the corbino disk (Reference 2) is

$$R_o = \frac{\rho_o}{2\pi d} \ln \left[\frac{r_2}{r_1}\right] \tag{1}$$

where

r_1 = inner radius of the corbino disk

r_2 = outer radius of the corbino disk

d = thickness

ρ_o = resistivity of the material when $B = 0$

R_o = resistance when $B = 0$

2.1.2 The Corbino Disk Magnetoresistance for a Single Conduction Band and a Spherical Energy Surface of Electrons

$$\left[\frac{\Delta\rho}{\rho_o}\right]_c = \frac{\rho_B - \rho_o}{\rho_o}$$

$$= \tan^2\theta$$

$$= (\mu_e B)^2 \tag{2}$$

In practice a number of factors may cause a departure of this characteristic from a B^2 dependence, particularly in high magnetic fields. Such factors are manifest in the form of physical magnetoresistance ($\Delta\rho/\rho_o$) such that the resistivity is no longer independent of the magnetic field. Wieder

(Reference 3) has shown that the corbino magnetoresistance is then expressed by

$$\left[\frac{\Delta\rho}{\rho_o}\right]_{p.c.} = \left[\frac{\Delta\rho}{\rho_o}\right]_c + \frac{\rho_B}{\rho_o}\tan^2\theta = \frac{\rho_B}{\rho_o}(1+\tan^2\theta) - 1 \tag{3}$$

2.1.3 Corbino Disk Magnetoresistance for Two Different Conduction Bands

$$\left[\frac{\Delta\rho}{\rho_o}\right]_c = \frac{\left(\mu_1^2\frac{\sigma_1}{\sigma_o} + \mu_2^2\frac{\sigma_2}{\sigma_o}\right)B^2 + (\mu_1\mu_2B^2)^2}{1 + \left(\mu_1^2\frac{\sigma_2}{\sigma_o} + \mu_2^2\frac{\sigma_1}{\sigma_o}\right)B^2} \tag{4}$$

where

μ_n = electron mobility

μ_p = hole mobility

μ_1, μ_2 = mobilities of each band

σ_1, σ_2 = zero field conductivities of each band

σ_o = effective zero field conductivity

In the low-field region (Reference 4), $\mu_n B << 1$ and we have

$$\left[\frac{\Delta\rho}{\rho_o}\right]_c \simeq \frac{9\pi}{16}(\mu_n B)^2 \tag{5}$$

In a stronger region, $\mu_n B \geq 1$

$$\left[\frac{\Delta\rho}{\rho_o}\right]_c \simeq \frac{9\pi}{16}(\mu_p B)^2 + b \tag{6}$$

where $b \equiv \mu_n/\mu_p$ and $b >> 1$ for InSb.

In the very strong field region, $\mu_p B >> 1$

$$\left[\frac{\Delta\rho}{\rho_o}\right]_c = \frac{9\pi}{32}\mu_n\mu_p B^2 \tag{7}$$

2.1.4 Magnetoresistance of Two-Layer Corbino Disks

A corbino disk is divided into two-layer disks (Reference 5), and the magnetoresistance of the disk is

$$\left[\frac{\Delta R}{R_o}\right]_c = \frac{R(B) - R_o}{R_o} = \frac{\mu_b^2 B^2}{1 + K(1+\mu_b^2 B^2)} \tag{8}$$

where

μ_b = thicker layer mobility

$K \equiv \frac{\text{surface-like sheet resistivity}}{\text{bulk-like sheet resistivity}}$

$= \frac{\sigma_s d_s}{\sigma_b d_b}$

σ_s = thin layer conductivity

d_s = thin layer thickness

σ_b = thicker layer conductivity

d_b = thicker layer thickness

2.1.5 MIS Thin-Film Transistor

The equations for the MIS thin-film transistor introduce the MIS magnetoresistance devices. In general, the source current in the simplified MIS transistor is expressed as

$$i_S = \frac{g_m E_i}{1 + g_m R_S} \tag{9}$$

where

i_S = source current

g_m = mutual conductance

E_i = input voltage

R_S = source resistance

The transconductance, g_m, is expressed as

$$g_m = \left.\frac{\Delta I_D}{\Delta V_{GS}}\right|_{V_{DS}}$$

$$= \frac{\varepsilon W \mu_d V_{DS}}{h_I \cdot L} \qquad (10)$$

where

I_D = drain current

V_{GS} = voltage between drain and source

ε = dielectric constant of the insulator

W = width of the dielectric material

L = length of the dielectric material

h_I = height of the dielectric material (insulator)

μ_d = effective drift mobility of the Δn electrons

The drain-source resistance of the MIS field-effect transistor R_{DS} is expressed as

$$R_{DS} = \frac{L \cdot h_I}{\varepsilon \cdot W \cdot \mu_d \cdot V_{GS}} \qquad (11)$$

If $V_{DS} = V_{GS}$, we obtain

$$R_{DS} = \frac{L \cdot h_I}{\varepsilon \cdot W \cdot \mu_d \cdot V_{DS}} \tag{12}$$

2.1.6 Magnetoresistance of the Rectangular Slab and MIS Device

$$R_S(B) = R_{SO} \frac{\rho_{SB}}{\rho_{SO}} (1+\mu_H^2 B^2)^{1/2} \tag{13}$$

where

$R_S(B)$ = slab resistance with magnetic field, B

ρ_{SB} = slab resistivity with magnetic field, B

ρ_{SO} = slab resistivity without magnetic field

μ_H = Hall mobility

B = applied magnetic field

R_{SO} = resistance of the slab when B = 0

For the MIS field-effect transistor,

$$R_S(B) = R_{DS}(B)$$

$$= \frac{L \cdot h_I}{\varepsilon \cdot W \cdot \mu_d \cdot V_{DS}} \frac{\rho_{SB}}{\rho_{SO}} (1+\mu_H^2 B^2)^{1/2} \tag{14}$$

$$R_S(B) = \frac{L \cdot h_I}{\varepsilon \cdot W \cdot \mu_d \cdot V_{DS}} \frac{\mu_o}{\mu_B} (1+\mu_H^2 B^2)^{1/2} \tag{15}$$

since

$$\frac{\rho_{SB}}{\rho_{SO}} = \frac{\mu_o}{\mu_B}$$

where

μ_o = mobility when B = 0

μ_B = mobility when B $\neq$ 0

2.1.7 MIS Corbino Disk

The zero-field drain-source resistance, R_{DSO}, is expressed as

$$R_{DSO} = \frac{\rho_o}{2\pi h_S} \ln \frac{r_2}{r_1} \quad (16)$$

The drain-source resistance of the MIS corbino disk is

$$[R_{DS}]_c = \frac{g_m}{I_D} \frac{h_I}{2\pi\varepsilon\mu_d} \ln \frac{r_2}{r_1}$$

$$= \frac{h_I}{2\pi\varepsilon\mu_d V_{GS}} \ln \frac{r_2}{r_1} \quad (17)$$

Since

$$g_m = \frac{I_D}{V_{GS}}$$

hence,

$$[R_{DS}]_c = R_{DSO} \frac{h_I h_S}{\rho_o \varepsilon \mu_d V_{GS}} \quad (18)$$

where

h_I = height of insulator (thickness)

h_S = height of semiconductor (thickness)

ρ_o = semiconductor resistivity when B = 0

V_{GS} = voltage between gate and source

2.1.8 MIS Corbino Disk Magnetoresistance

a. For $V_{GS} = 0$ and $B = 0$

$$[R_{DS}]_{VO,BO} = \frac{\rho_o}{2\pi h_S} \ln \frac{r_2}{r_1} \tag{19}$$

b. For $V_{GS} \neq 0$ and $B = 0$

$$[R_{DS}]_{V,BO} = [R_{DS}]_{VO,BO} // R_{MIS}$$

$$= \frac{\rho_o}{2\pi} \left[\ln \frac{r_2}{r_1} \right] \frac{h_I}{h_I h_S + \rho_o \varepsilon \mu_d V_{GS}} \tag{20}$$

where

$$R_{MIS} = \frac{h_I h_S}{\varepsilon \rho_o \mu_d V_{GS}} [R_{DS}]_{VO,BO}$$

c. For $V_{GS} \neq 0$ and $B \neq 0$

$$[R_{MIS}(B)]_c = [R_{DS}]_{V,BO} // R(B) \tag{21}$$

where R(B) = magnetic field-dependent resistance of two-layer corbino disk.

$$R(B) = \frac{\rho_b (1+\mu_b^2 B^2)}{2\pi d_b [1+K(1+\mu_b^2 B^2)]} \ln \frac{r_2}{r_1} \tag{22}$$

and

$$R(O) = \frac{\rho_b}{2\pi d_b(1+K)} \ln \frac{r_2}{r_1} \tag{23}$$

Hence,

$$[R_{MIS}(B)]_c = \frac{\rho_b(1+\mu_b^2B^2)\ln\frac{r_2}{r_1}}{2\pi\left[h_b+\left(Kh_b+\frac{\rho_b}{\rho_o}h_S+\frac{\rho_b\varepsilon\mu_d V_{GS}}{h_I}\right)(1+\mu_b^2B^2)\right]} \tag{24}$$

and

$$[R_{MIS}(O)]_c = \frac{\rho_b \ln\frac{r_2}{r_1}}{2\pi\left[h_b+\left(Kh_b+\frac{\rho_b}{\rho_o}h_S+\frac{\rho_b\varepsilon\mu_d V_{GS}}{h_I}\right)\right]} \tag{25}$$

Finally, the magnetoresistance of the MIS corbino disk is expressed as

$$\left[\frac{\Delta R_{MIS}}{R_{MIS}(O)}\right]_c = \frac{\mu_b^2B^2}{1+\left(K+\frac{\rho_b h_S}{\rho_o h_b}+\frac{\rho_b\varepsilon\mu_d V_{GS}}{h_I h_b}\right)(1+\mu_b^2B^2)} \tag{26}$$

where

μ_b = thicker layer mobility

ρ_b = thicker layer resistivity

h_b = thickness of thicker layer

h_I = thickness of insulator

h_S = thickness of semiconductor

2.2 Calculations of the Magnetoresistance of the MIS Devices

2.2.1 Material Properties (References 4 and 5)

Material	InSb-8n, Ohio Semicon., Inc.
Type of semiconductor	n-type
Maximum electron concentration at 80°K	5×10^{14} atoms/cm^3
Minimum mobility at 80°K	300,000 cm^2/V-sec
Energy gap at 300°K	0.16 eV
Resistivity at 80°K	$\rho_o = \frac{1}{q\mu_e n} = 0.041$ ohm-cm
Resistivity at 300°K	0.003-0.005 ohm-cm
Mobility at 300°K	78,000 cm^2/V-sec for the concentration of 5×10^{14} cm^{-3}

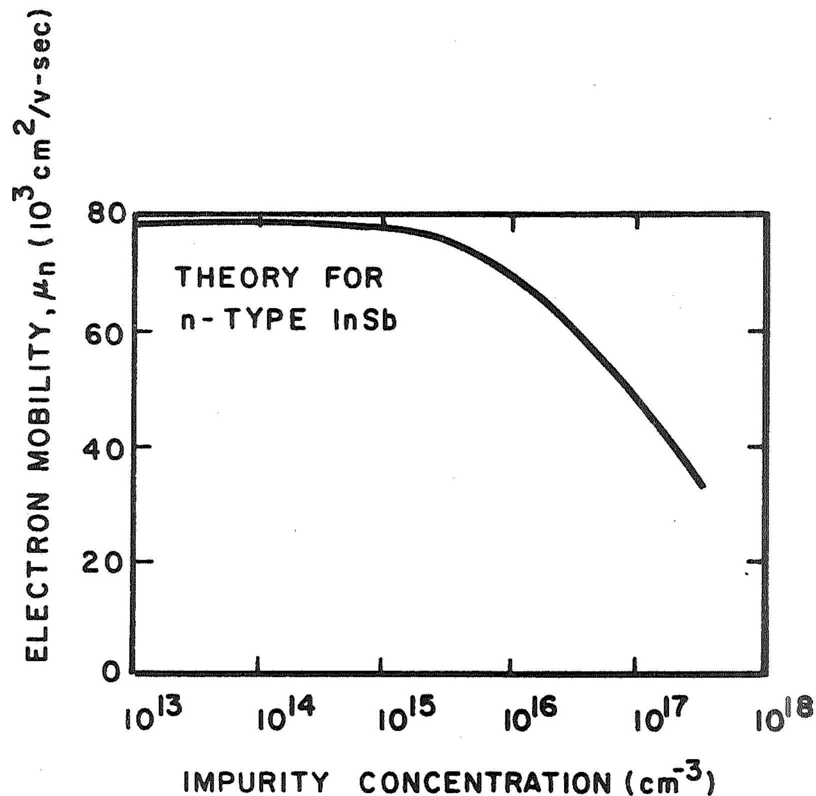

Figure 1. Dependence of electron mobility on impurity concentration for n-type InSb at room temperature (Reference 6)

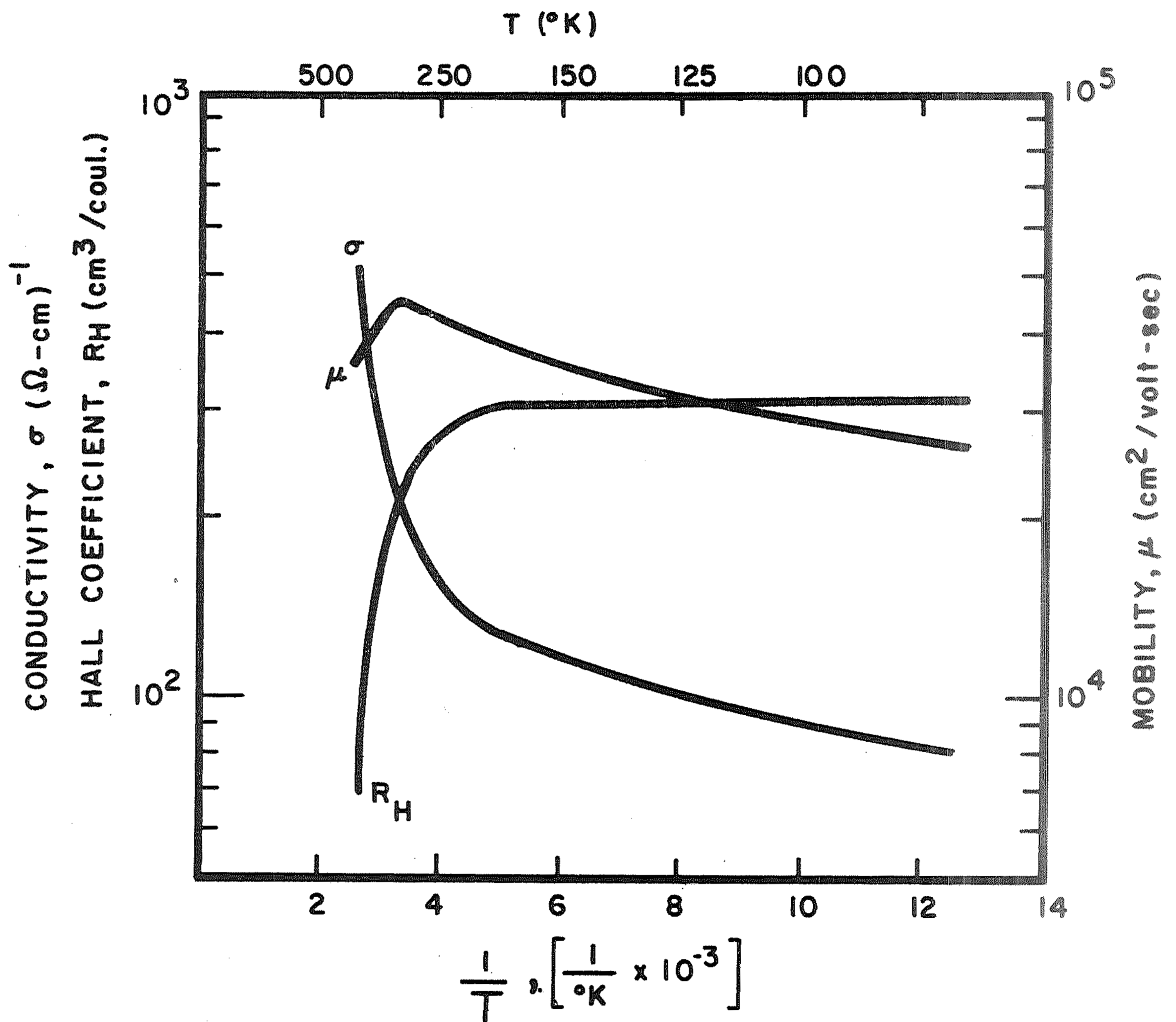

Figure 2. Temperature vs. mobility, Hall coefficient and conductivity for InSb thin films (Reference 7)

2.2.2 Resistance of the Corbino Disk

From Equation 1 we obtain

$$R_o = \frac{\rho_o}{2\pi d} \ln \frac{r_2}{r_1}$$

$$= \frac{0.004}{2\pi \cdot 0.1} \ln \frac{0.4}{0.1} \text{ (ohms)}$$

$$= 8.8 \times 10^{-3} \text{ ohm} \qquad (27)$$

since

$r_2 = 0.4$ cm

$r_1 = 0.1$ cm

$d = 0.1$ cm

$\rho_o = 0.004$ ohm-cm

2.2.3 The Corbino Disk Magnetoresistance for a Single Conduction Band and a Spherical Energy Surface of Electrons

From Equation 3 we have

$$\left[\frac{\Delta\rho}{\rho_o}\right]_{p.c.} = \frac{\rho_B}{\rho_o}(1+\tan^2\theta) - 1$$

$$= \frac{\rho_B}{\rho_o}(1+\mu^2B^2) - 1$$

$$= \frac{\rho_o(1+\mu^2B^2)(1+\mu^2B^2)}{\rho_o} - 1$$

$$= (1+\mu^2B^2)^2 - 1$$

Substituting $\mu_n = 78,000\ cm^2/V\text{-}sec$ and plotting $[\Delta\rho/\rho_o]_{p.c.}$ with respect to field B, we have a curve as shown in Figure 3.

2.2.4 The Corbino Disk Magnetoresistance for Two Different Conduction Bands

a. $\mu_n B << 1$ (low-field region)

For this region, $B << 1000$ gauss

$$\left[\frac{\Delta\rho}{\rho_o}\right] \simeq \frac{9\pi}{16}(\mu_n B)^2$$

$$= 108B^2 \text{ where } \mu_n = 7.8\ m^2/V\text{-sec.}$$

The curve is plotted in Figure 4.

B (gauss)	$\left[\frac{\Delta\rho}{\rho_o}\right]$ for $\mu_n B << 1$
0	0
1	1.08×10^{-6}
10	1.08×10^{-4}
50	2.70×10^{-3}
100	1.08×10^{-2}
200	4.32×10^{-2}
400	1.73×10^{-1}
500	2.70×10^{-1}

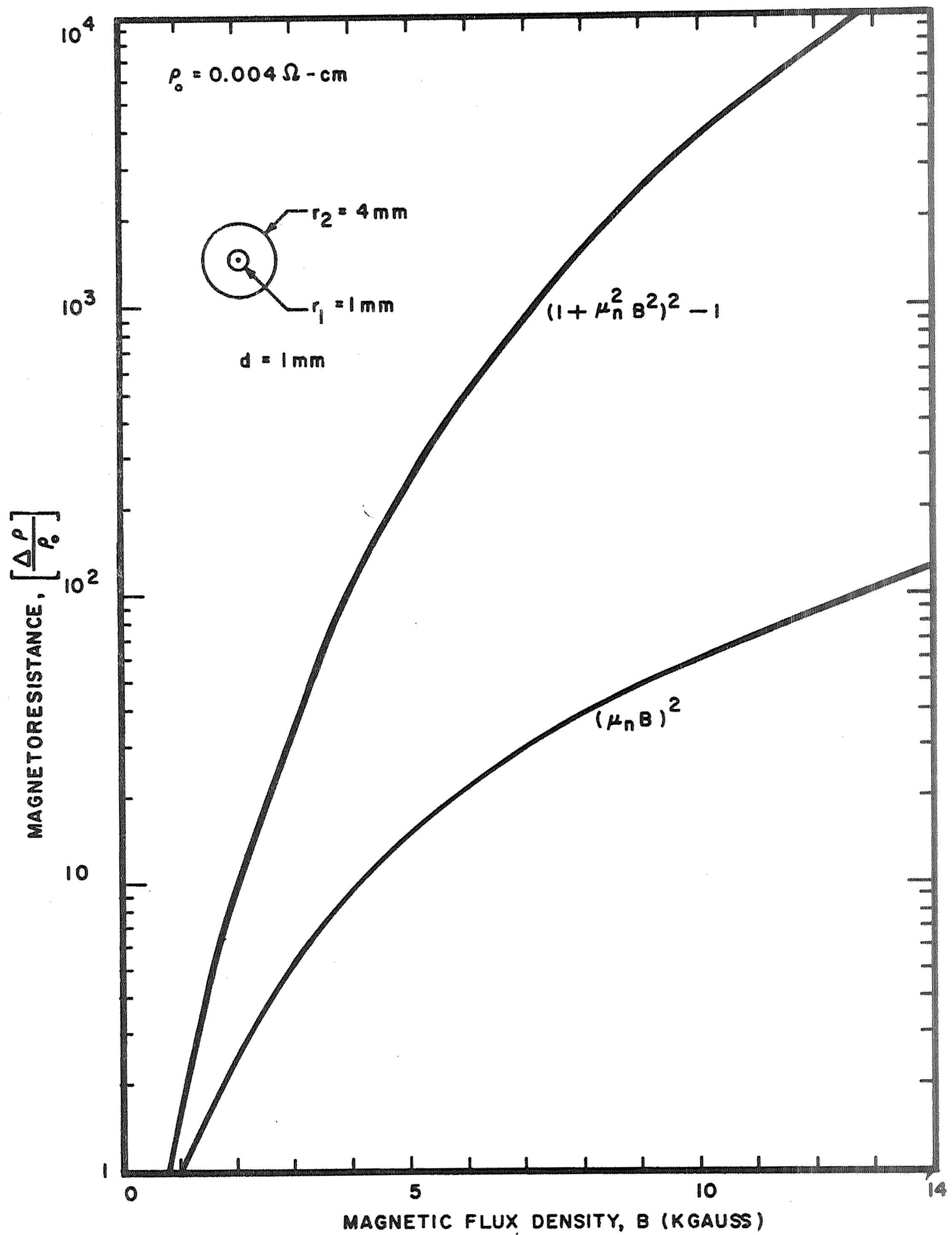

Figure 3. Corbino disk magnetoresistance vs. magnetic induction B

b. $\mu_n B \geq 1$ (a stronger region)

$$\left[\frac{\Delta\rho}{\rho_o}\right]_c \simeq \frac{9\pi}{16}(\mu_p B)^2 + b$$

$$= 1.68 \times 10^{-2} B^2 + 80$$

where

$b = 80$

$\mu_p = 975\ cm^2/V\text{-}sec$ (700 $cm^2/V\text{-}sec$ by Madelung)

B (kilogauss)	$\left(\frac{\Delta\rho}{\rho_o}\right)$ for $\mu_n B \geq 1$
0	-
1	$1.68 \times 10^{-4} + 80$
2	$6.70 \times 10^{-4} + 80$
3	$1.51 \times 10^{-3} + 80$
4	$2.68 \times 10^{-3} + 80$
5	$4.20 \times 10^{-3} + 80$
6	$6.05 \times 10^{-3} + 80$
8	$1.07 \times 10^{-2} + 80$
10	$1.68 \times 10^{-2} + 80$
100	$1.68 + 80$
200	$6.72 + 80$
500	$42.00 + 80$
1000	$168.00 + 80$

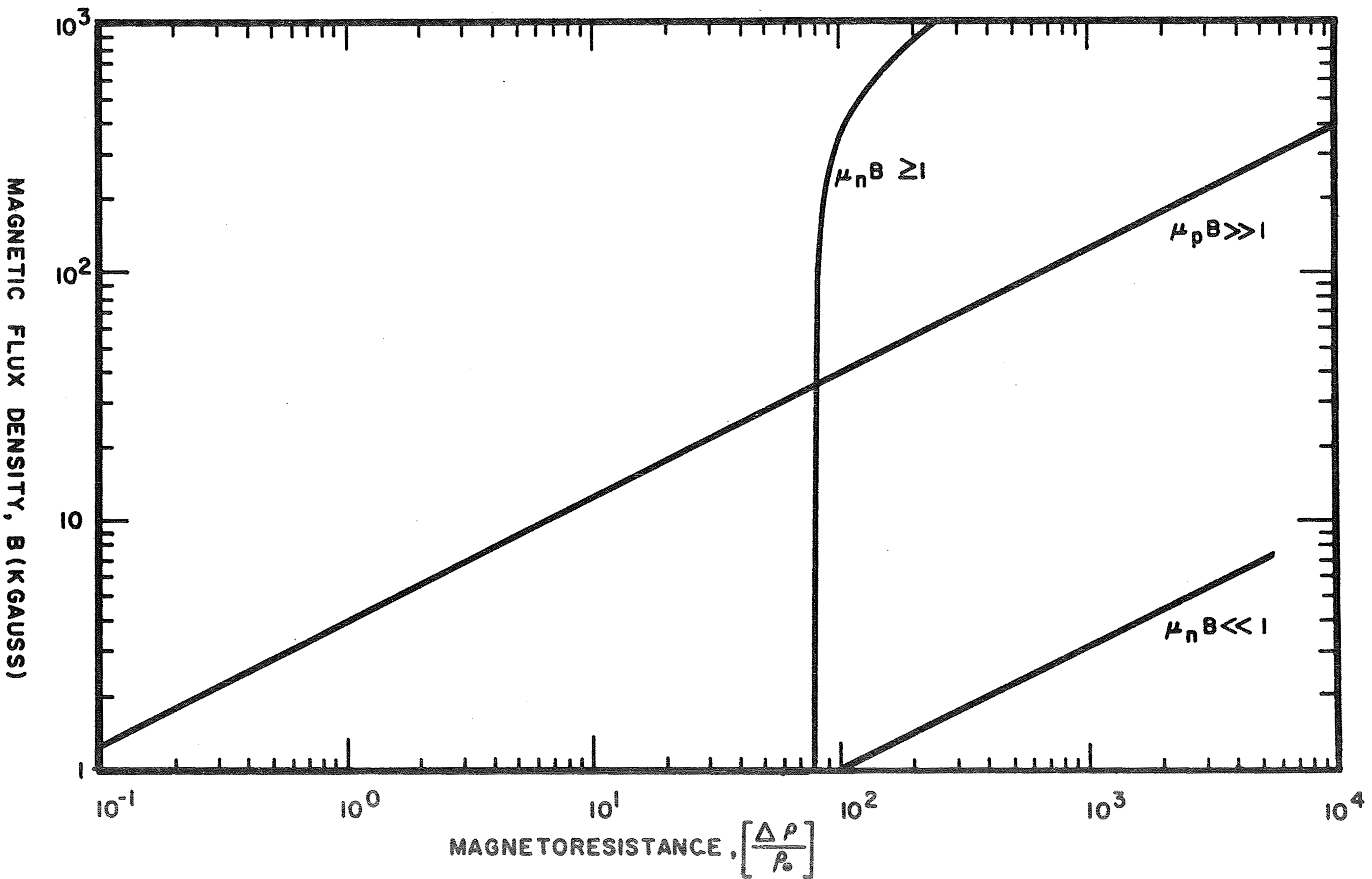

Figure 4. Corbino disk magnetoresistance for two conduction bands vs. magnetic flux density (strong field)

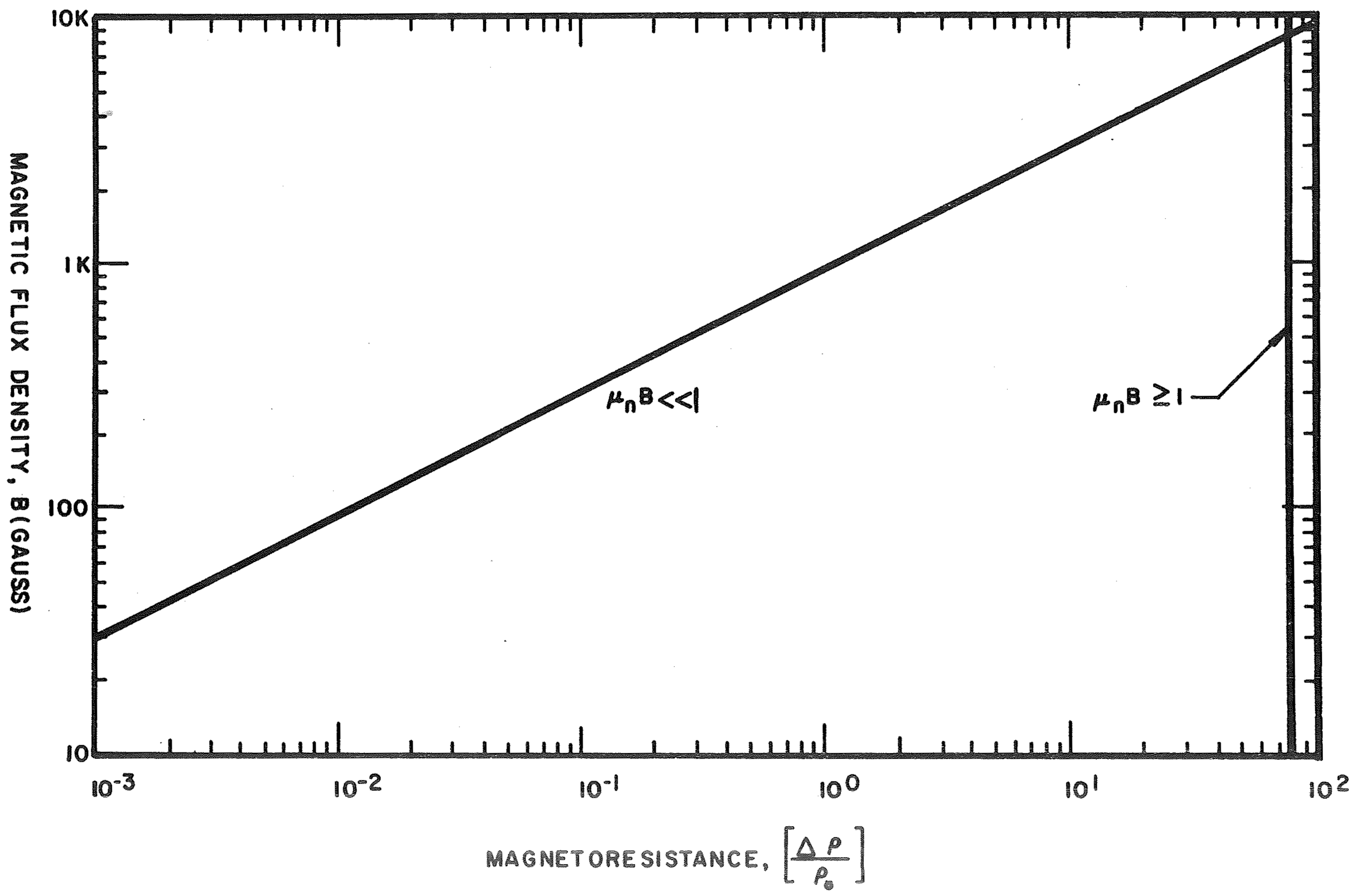

Figure 5. Corbino disk magnetoresistance for two conduction bands vs. magnetic flux density (low field)

c. $\mu_p B >> 1$ (very strong field region)

$$\left(\frac{\Delta\rho}{\rho_o}\right)_c \simeq \frac{9\pi}{32}\mu_n\mu_p B^2$$

$$= 8.83 \times 7.8 \times 0.0975 \times B^2$$

$$= 6.71B^2$$

B (kilogauss)	$\left(\frac{\Delta\rho}{\rho_o}\right)$ for $\mu_p B >> 1$
10	6.71
20	26.85
50	167.50
70	329.00
100	671.00
200	2,685.00
300	6,040.00
400	10,740.00
500	16,750.00

2.2.5 Magnetoresistance of Two-Layer Corbino Disks

Let

$\mu_b = 78,000\ cm^2/V\text{-}sec$

σ_s = surface conductivity

σ_b = bulk conductivity

d_s = surface thickness

d_b = bulk thickness

$$K = \frac{\sigma_s d_s}{\sigma_b d_b} \simeq 0.03$$

$$\left[\frac{\Delta R}{R_o}\right]_c \simeq \frac{\mu_b^2 B^2}{1 + K(1+\mu_b^2 B^2)}$$

$$= \frac{60.84B^2}{1.03 + 1.825B^2}$$

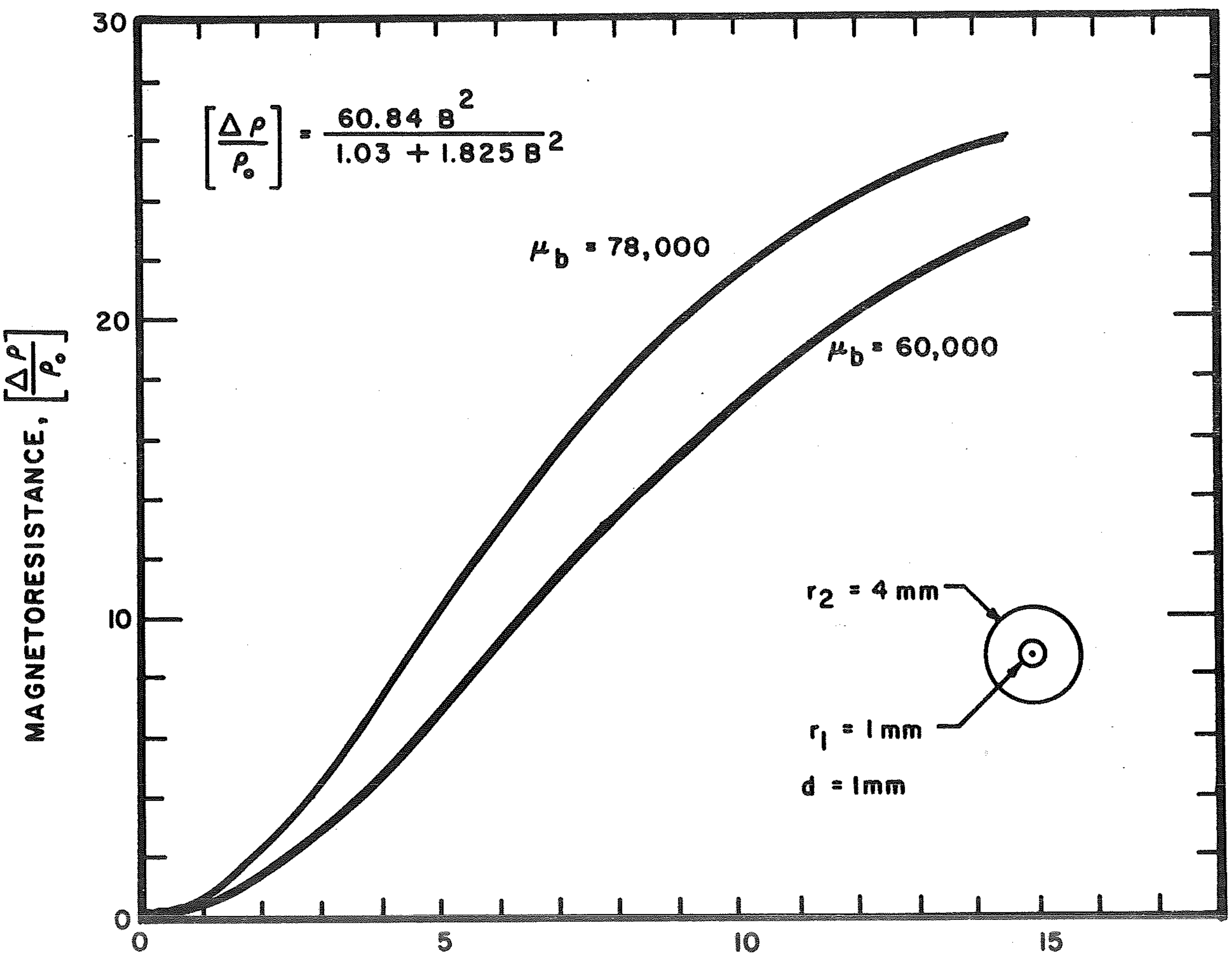

Figure 6. Magnetoresistance of two-layer corbino disks vs. magnetic flux density

B (kilogauss)	$\left[\frac{\Delta\rho}{\rho_o}\right] = \mu_b^2 B^2/1 + K(1+\mu_b^2 B^2)$
0	0
1	0.581
2	2.202
4	7.360
6	12.980
8	17.700
10	21.350
12	24.100
14	25.700

If we let $\mu_b = 60,000\ cm^2/V\text{-}sec$ (= $6\ m^2/V\text{-}sec$)

$$\left[\frac{\Delta R}{R_o}\right]_c \approx \frac{36B^2}{1.03 + 3.10^{-2} \cdot 36B^2}$$

B (kilogauss)	$\left[\frac{\Delta\rho}{\rho_o}\right]$ when $\mu_b = 60,000$
0	0.00
1	0.336
2	1.38
4	4.79
6	9.13
8	13.40
10	17.05
12	20.05
14	22.45
16	-

2.2.6 MIS Thin-Film Transistor

Let

$\varepsilon = K\varepsilon_o = 100 \cdot 0.09\ pf/cm = 9 \times 10^{-10}$ farad/cm

$h_I = 0.1\ \mu m = 10^{-7}\ m$

$L = 3\ \mu m = 3 \times 10^{-6}\ m$

$W = 625\ \mu m = 6.25 \times 10^{-4}\ m$

$$\mu_d = \mu_H \frac{n_F}{n_F + n_T}$$

In wide bandgap materials, we assume that the drift mobility μ_d is a constant independent of variations in gate voltage V_G. When the semiconductor contains many traps or surface states, the large fraction of trapped electrons may cause the effective drift mobility to be much smaller than the microscopic or Hall mobility by the factor θ (Reference 8)

$$\mu_d = \mu_D \theta = \mu_D \frac{n_F}{n_F + n_T}$$

where

μ_d = effective drift mobility in the presence of traps

μ_D = true drift mobility, assumed equal to the Hall mobility

n_F = free carrier density

n_T = density of trapped carriers

As the gate bias is further increased, most of the available traps are filled, resulting in much larger increases in conductivity of the semiconductor. Under these conditions, the drift mobility μ_d should approach a constant value equal to the Hall mobility ($\theta = 0$) and g_m should become a constant independent of gate bias. Therefore, we let $\mu_d \simeq \mu_H$. Then we have

$$g_m = \frac{\varepsilon \cdot W \cdot \mu_d V_{DS}}{h_I L}$$

$$= \frac{(9 \times 10^{-10})(6.25 \times 10^{-4})(7.8)(V_{DS})}{(10^{-7})(3 \times 10^{-6})}$$

$$= 15.6 V_{DS} \text{ ohm}^{-1}$$

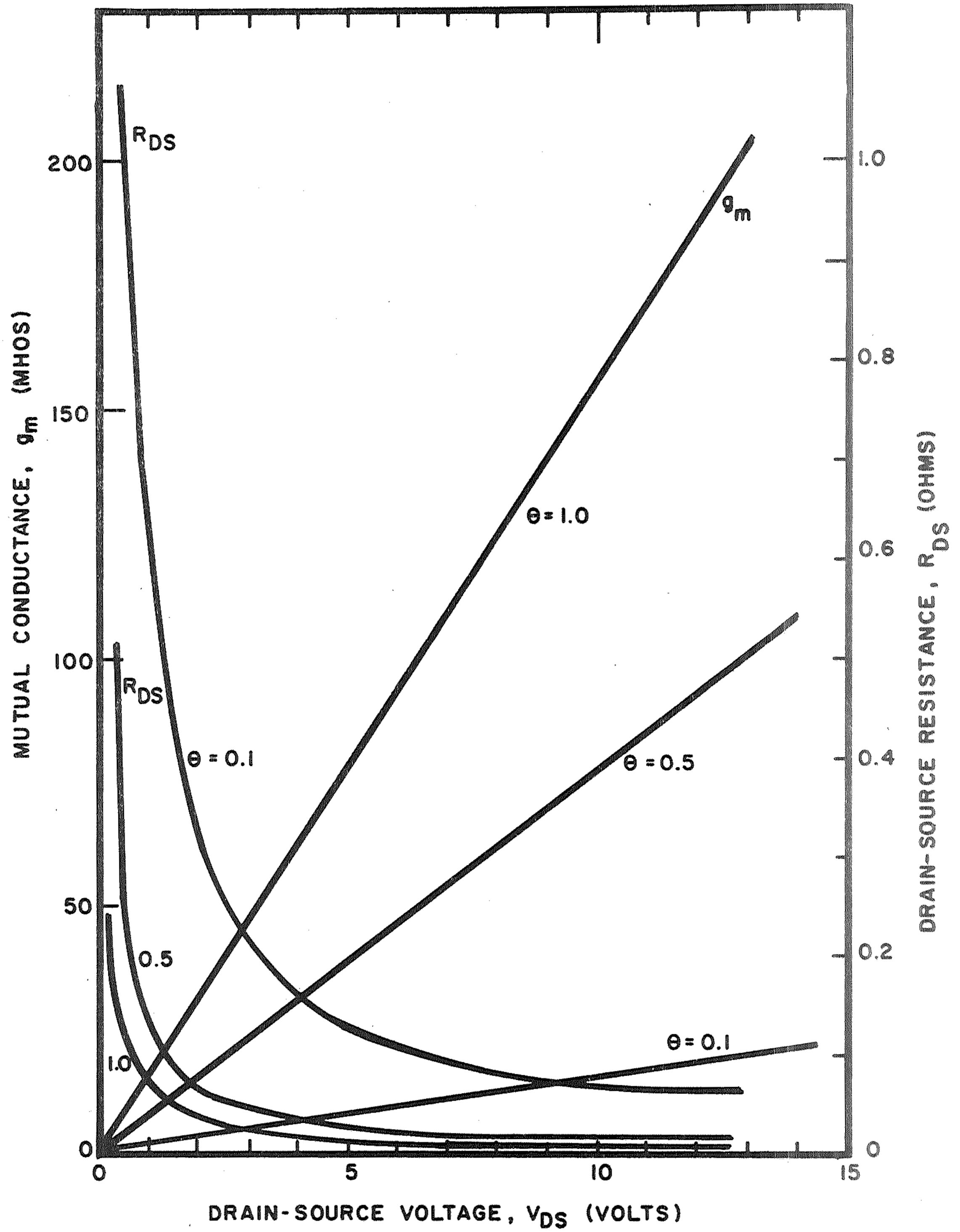

Figure 7. Mutual conductances and drain-source resistance vs. drain-source voltage

For $\theta = 0.5$,

$$g_m = 7.80 V_{DS} \text{ ohm}^{-1}$$

For $\theta = 0.1$,

$$g_m = 1.56 V_{DS} \text{ ohm}^{-1}$$

The drain-source resistance, R_{DS}, is as follows:

For $\theta = 1$,

$$R_{DS} = \frac{0.064}{V_{DS}} \text{ ohm}$$

For $\theta = 0.5$,

$$R_{DS} = \frac{0.128}{V_{DS}} \text{ ohm}$$

For $\theta = 0.1$,

$$R_{DS} = \frac{0.64}{V_{DS}} \text{ ohm}$$

2.2.7 Magnetoresistance of the Rectangular Slab and MIS Device

From Equation 13 and letting

μ_o = refer to Table I

μ_B = refer to Table I

μ_H = 78,000 cm^2/V-sec

$L = 3 \times 10^{-6}$ m

$W = 6.25 \times 10^{-4}$ m

$h_I = 10^{-7}$ m

$\mu_d = 78{,}000\ cm^2/V\text{-}sec = 7.8\ m^2/V\text{-}sec$

$\varepsilon = 9 \times 10^{-10}$ farad/m

V_{DS} = variable

$$R_S(B) = \frac{L \cdot h_I}{\varepsilon \cdot W \cdot \mu_d \cdot V_{DS}} \frac{\mu_o}{\mu_B}(1+\mu_H^2 B^2)^{1/2}$$

$$= \frac{0.064}{\theta V_{DS}} \frac{\mu_o}{\mu_B}(1+\mu_H^2 B^2)^{1/2}$$

From the table (Reference 9)

TABLE I

Comparison of μ_o/μ_B versus B

B (KG)	2	4	6	8	10
μ_o/μ_B (Weiss & Walker)	1.05	1.14	1.25	1.36	1.48
μ_o/μ_B (Simmons)	1.04	1.10	1.20	1.34	1.49

For $\theta = 1$,

$$R_S(B) = \frac{0.064}{V_{DS}} \cdot \frac{\mu_o}{\mu_B}(1+61 x B^2)^{1/2}$$

B (Kgauss)	$R_S(B)$
1	$0.064 \times 1.30/V_{DS} = 0.0832/V_{DS}$
2	$0.064 \times 1.945/V_{DS} = 0.1245/V_{DS}$
4	$0.064 \times 3.73/V_{DS} = 0.239/V_{DS}$
6	$0.064 \times 6.00/V_{DS} = 0.384/V_{DS}$
8	$0.064 \times 8.60/V_{DS} = 0.550/V_{DS}$
10	$0.064 \times 11.65/V_{DS} = 0.745/V_{DS}$
12	$0.064 \times 15.35/V_{DS} = 0.983/V_{DS}$

For $\theta = 0.5$

$$R_S(B) = \frac{0.128}{V_{DS}} \cdot \frac{\mu_o}{\mu_B}(1+61xB^2)^{1/2}$$

B (Kgauss)	R_S(B)
1	$0.1664/V_{DS}$
2	$0.2490/V_{DS}$
4	$0.4780/V_{DS}$
6	$0.7680/V_{DS}$
8	$1.1000/V_{DS}$
10	$1.4900/V_{DS}$
12	$1.9200/V_{DS}$

For $\theta = 0.1$

$$R_S(B) = \frac{0.64}{V_{DS}} \cdot \frac{\mu_o}{\mu_B}(1+61xB^2)^{1/2}$$

B (Kgauss)	R_S(B)
1	$0.832/V_{DS}$
2	$1.245/V_{DS}$
4	$2.390/V_{DS}$
6	$3.840/V_{DS}$
8	$5.500/V_{DS}$
10	$7.450/V_{DS}$
12	$9.800/V_{DS}$

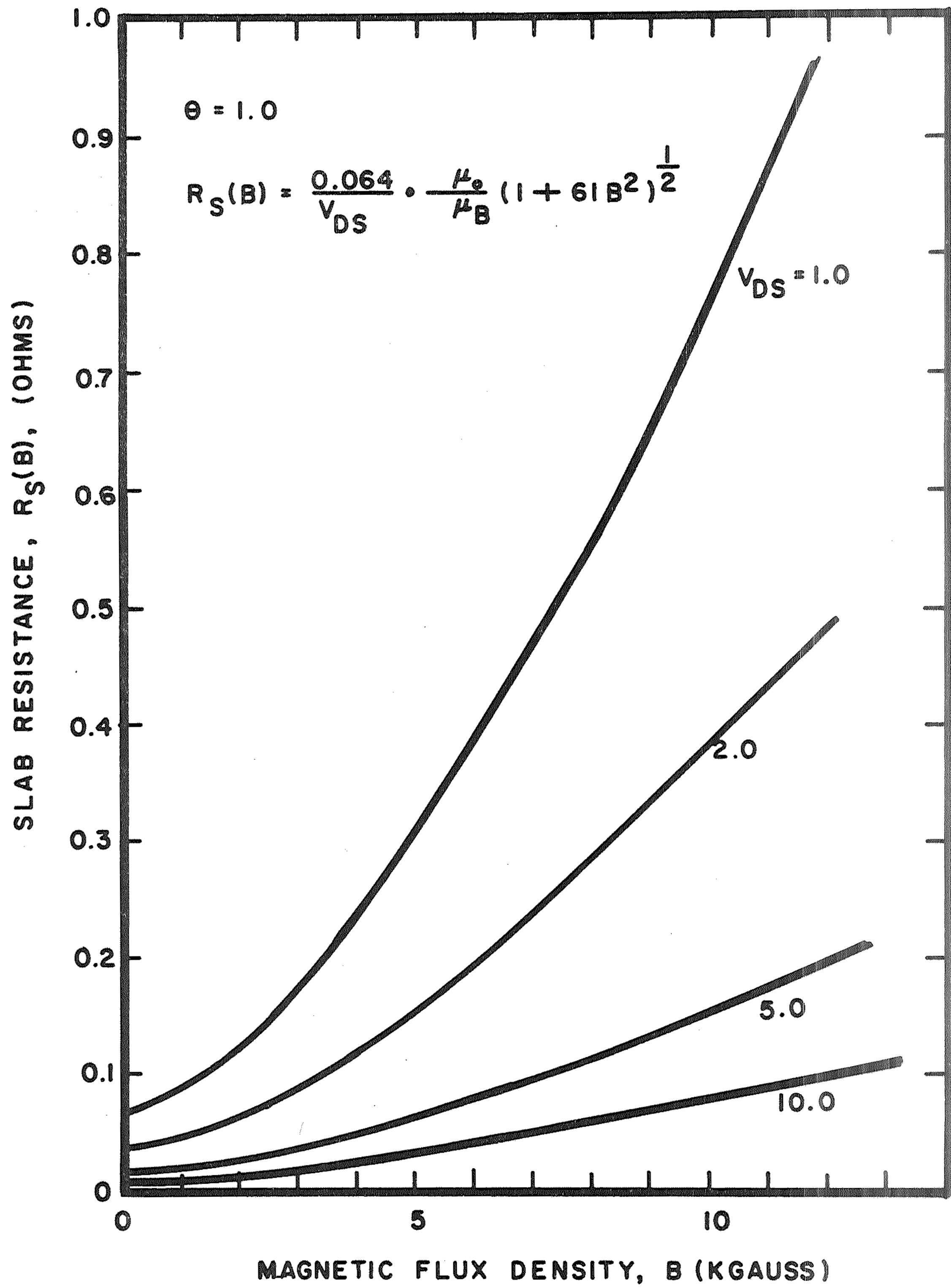

Figure 8. MIS slab resistance vs. magnetic flux density when θ = 1.0

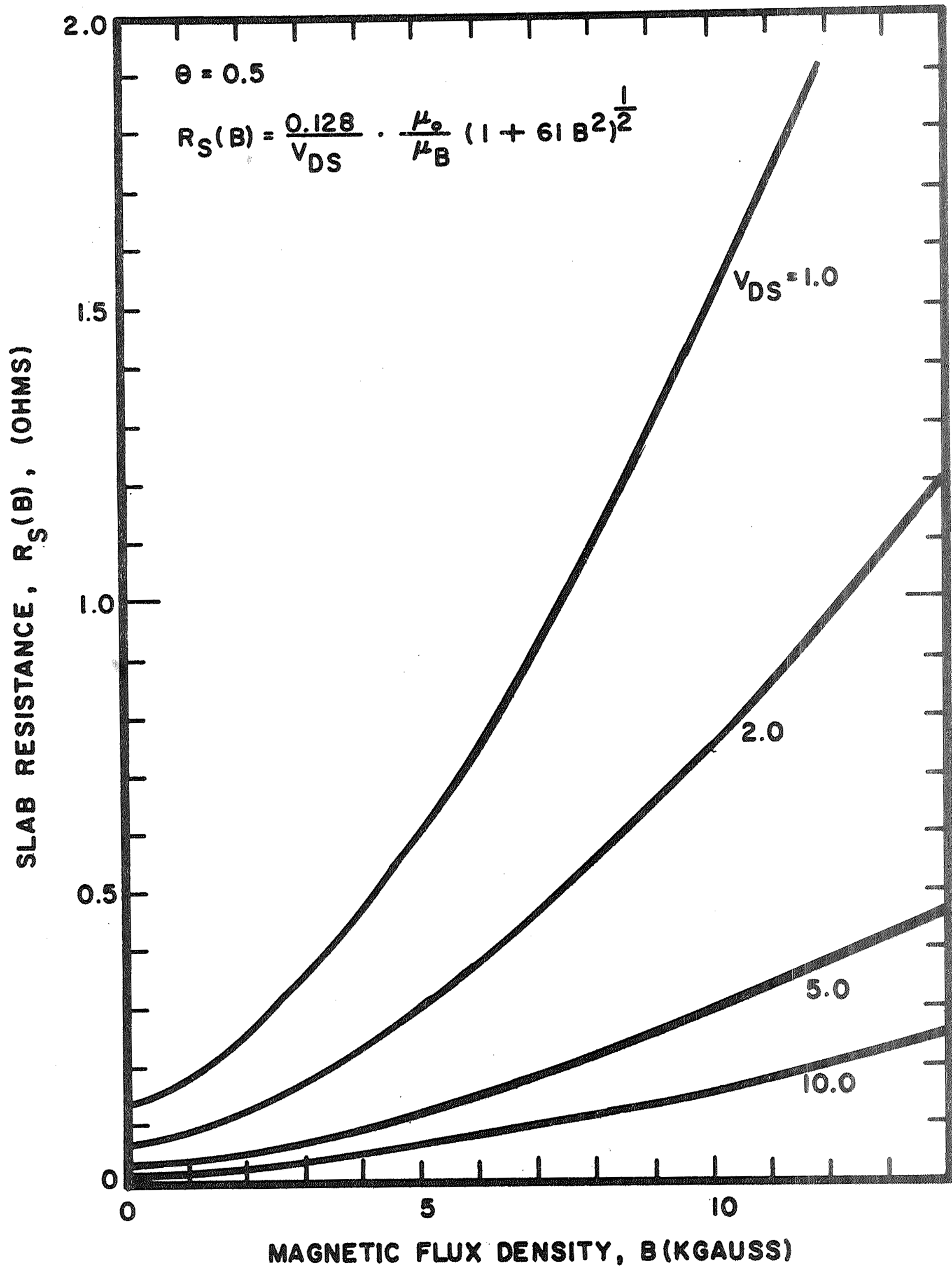

Figure 9. MIS slab resistance vs. magnetic flux density when θ = 0.5

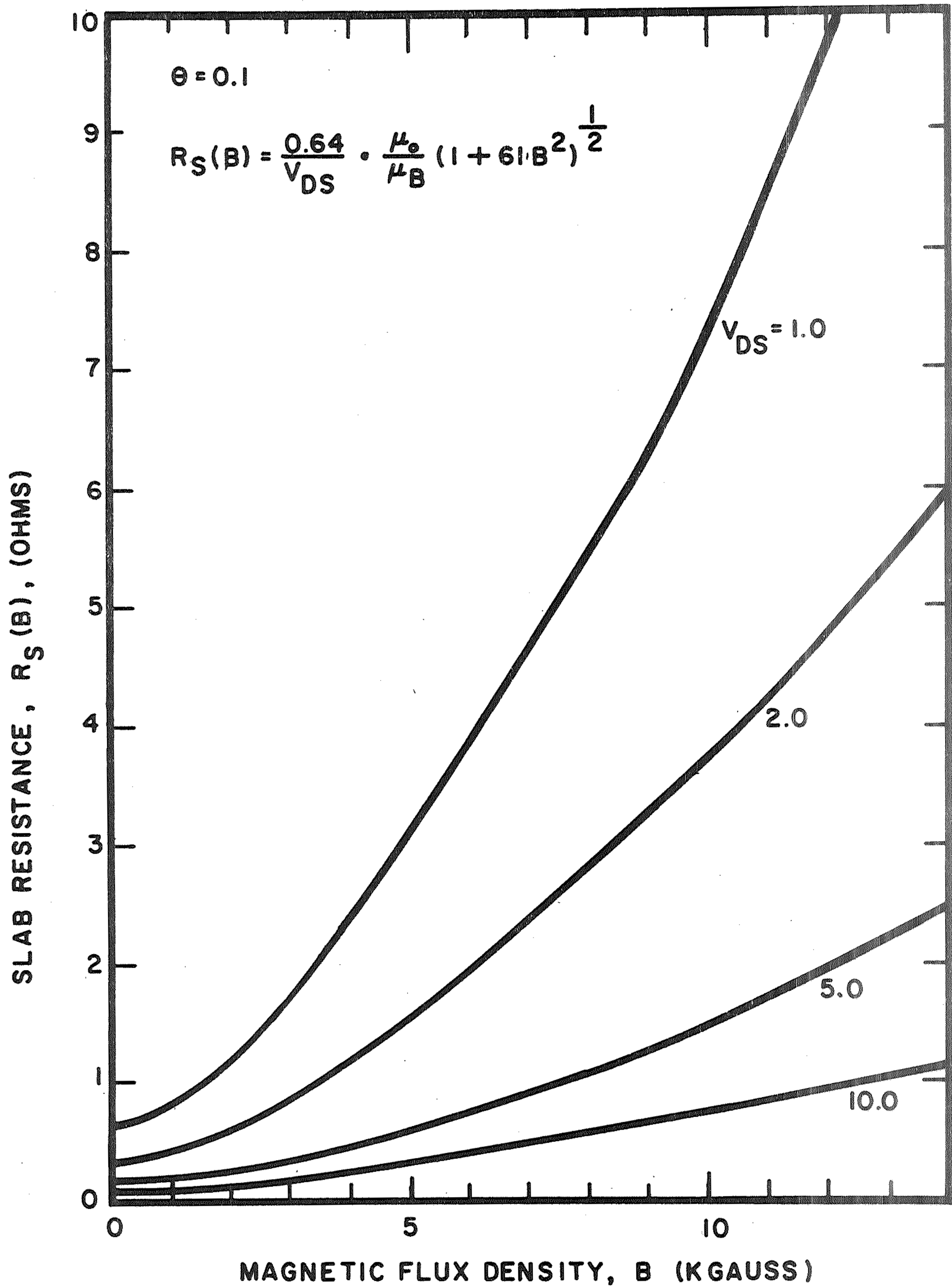

Figure 10. MIS slab resistance vs. magnetic flux density when θ = 0.1

2.2.8 MIS Corbino Disk

From Equation 16 and letting

$r_1 = 10^{-3}$ m

$r_2 = 4 \times 10^{-3}$ m

$h_S = 5 \times 10^{-6}$ m

$\rho_o = 4 \times 10^{-5}$ ohm-m

$$R_{DSO} = \frac{(4x10^{-5})}{2\pi(5x10^{-6})} \ln \frac{4x10^{-3}}{10^{-3}}$$

$$= 1.763 \text{ (ohms)}$$

$$[R_{DS}]_c = 1.763 \cdot \frac{h_I h_S}{\rho_o \varepsilon \mu_d V_{GS}}$$

$$= \frac{1.763 \cdot (10^{-7}) \cdot (5x10^{-6})}{(4x10^{-5})(9x10^{-10})(7.8\theta)V_{GS}}$$

$$= \frac{3.14}{\theta V_{GS}}$$

	$\theta = 1.0$	$\theta = 0.5$	$\theta = 0.1$
V_{GS}	$[R_{DS}]_c = \frac{31.4}{V_{GS}}\ \Omega$	$[R_{DS}]_c = \frac{6.28}{V_{GS}}\ \Omega$	$[R_{DS}]_c = \frac{31.4}{V_{GS}}\ \Omega$
1	3.140	6.28	31.40
2	1.570	3.14	15.70
4	0.785	1.57	7.85
6	0.524	1.045	5.24
8	0.393	0.785	3.93
10	0.314	0.628	3.14

2.2.9 MIS Corbino Disk Magnetoresistance

From Equations 19, 20, and 24 and letting

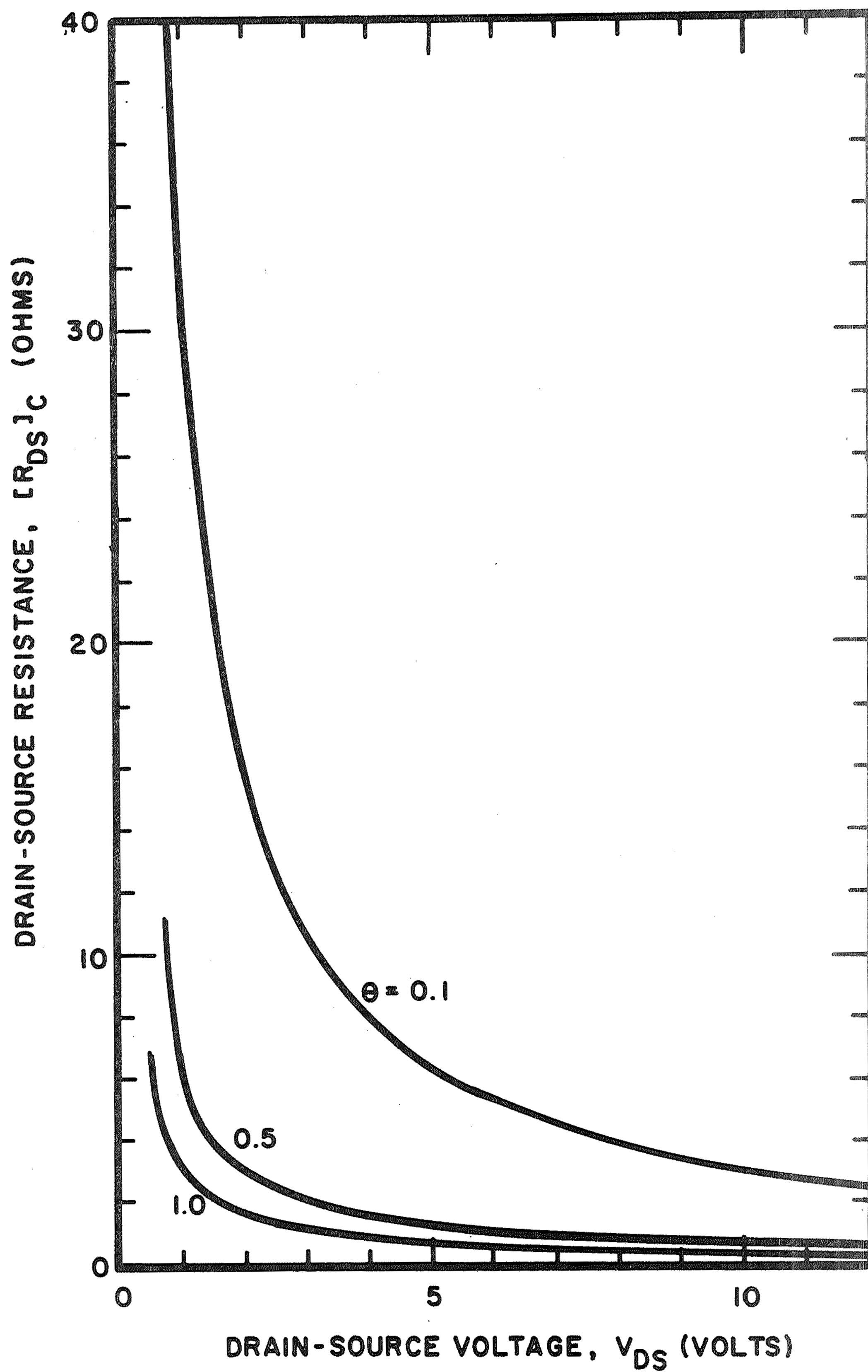

Figure 11. MIS corbino disk drain-source resistance vs. drain-source voltage

$$r_1 = 10^{-3} \text{ m}$$

$$r_2 = 4 \times 10^{-3} \text{ m}$$

$$h_S = 5 \times 10^{-6} \text{ m}$$

$$\rho_o = 4 \times 10^{-5} \text{ ohm-m}$$

$$h_I = 10^{-7} \text{ m}$$

$$\varepsilon = 9 \times 10^{-10} \text{ (for Ti)}$$

$$\mu_d = \mu_H \theta = 7.8\theta \text{ m}^2/\text{V-sec}$$

$$V_{GS} = \text{variable}$$

$$(R_{DS})_{VO,BO} = \frac{4 \times 10^{-5}}{2\pi \times 5 \times 10^{-6}} \ln \frac{4}{1} = 1.763 \text{ ohms}$$

$$(R_{DS})_{V,BO} = (R_{DS})_{VO,BO} \frac{1}{1 + \left(\frac{\rho_o \varepsilon \mu_d V_{GS}}{h_I h_S}\right)}$$

$$= \frac{1.763}{1 + \frac{(4\text{x}10^{-5})(9\text{x}10^{-10})(7.8\theta)V_{GS}}{(10^{-7})(5\text{x}10^{-6})}}$$

$$= \frac{1.763}{1 + 0.561\theta V_{GS}}$$

	$\theta = 1.0$	$\theta = 0.5$	$\theta = 0.1$
		$(R_{DS})_{V,BO} =$	
V_{GS}	$\frac{1.763}{1 + 0.561V_{GS}}$	$\frac{1.763}{1 + 0.281V_{GS}}$	$\frac{1.763}{1 + 0.0561V_{GS}}$
0	1.763	1.763	1.763
1	1.130	1.375	1.670
2	0.832	1.130	1.584
4	0.545	0.832	1.440
6	0.404	0.656	1.320
8	0.322	0.545	1.218
10	0.267	0.463	1.130

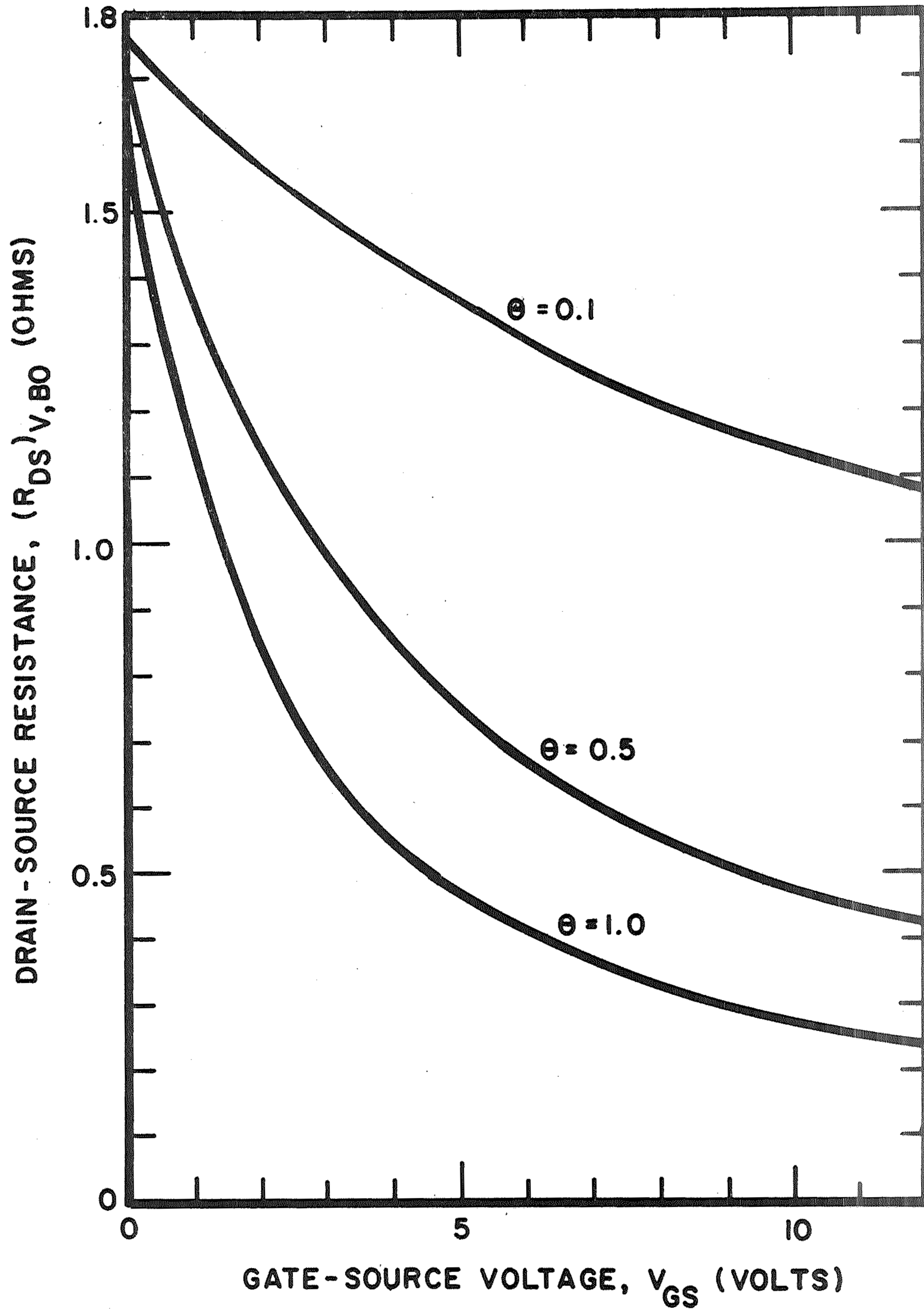

Figure 12. Drain-source resistance vs. gate-source voltage as a function of θ

Letting

$$\mu_b = \mu_H = 7.8 \ m^2/V\text{-sec or } 6.0 \ m^2/V\text{-sec}$$

$$K = \frac{\sigma_s d_s}{\sigma_b d_b} \simeq 0.03$$

$$\varepsilon = 9 \times 10^{-10} \text{ farad}$$

$$\mu_d = \theta\mu_H = 7.8\theta \ m^2/V\text{-sec}$$

$$h_I = 10^{-7} \ m$$

$$h_S = 5 \times 10^{-6} \ m$$

$$\rho_o = 4 \times 10^{-5} \text{ ohm-m}$$

$$h_b \simeq h_S = 5 \times 10^{-6} \ m$$

$$\rho_b \simeq \rho_o = 4 \times 10^{-5} \text{ ohm-m}$$

$$\left[\frac{\Delta R_{MIS}}{R_{MIS}(O)}\right]_C \simeq \frac{61B^2}{1 + \left(K+1+\frac{\rho_o \varepsilon \mu_d V_{GS}}{h_I h_S}\right)(1+61B^2)}$$

$$= \frac{61B^2}{1 + (1.03+0.561\theta V_{GS})(1+61B^2)}$$

	$\theta = 1.0$		
	$V_{GS} = 1.0$	$V_{GS} = 2.0$	$V_{GS} = 5.0$
B (Kgauss)	$MR = \frac{61B^2}{2.591+97B^2}$	$MR = \frac{61B^2}{3.15+131B^2}$	$MR = \frac{61B^2}{4.835+233.9B^2}$
0	0	0	0
0.5	0	0.0439	0.0280
1	0.171	0.1425	0.0850
2	0.377	0.2915	0.1730
4	0.539	0.405	0.2320
6	0.584	0.435	0.2466
8	0.612	0.450	0.2526
10	0.614	0.455	0.2555

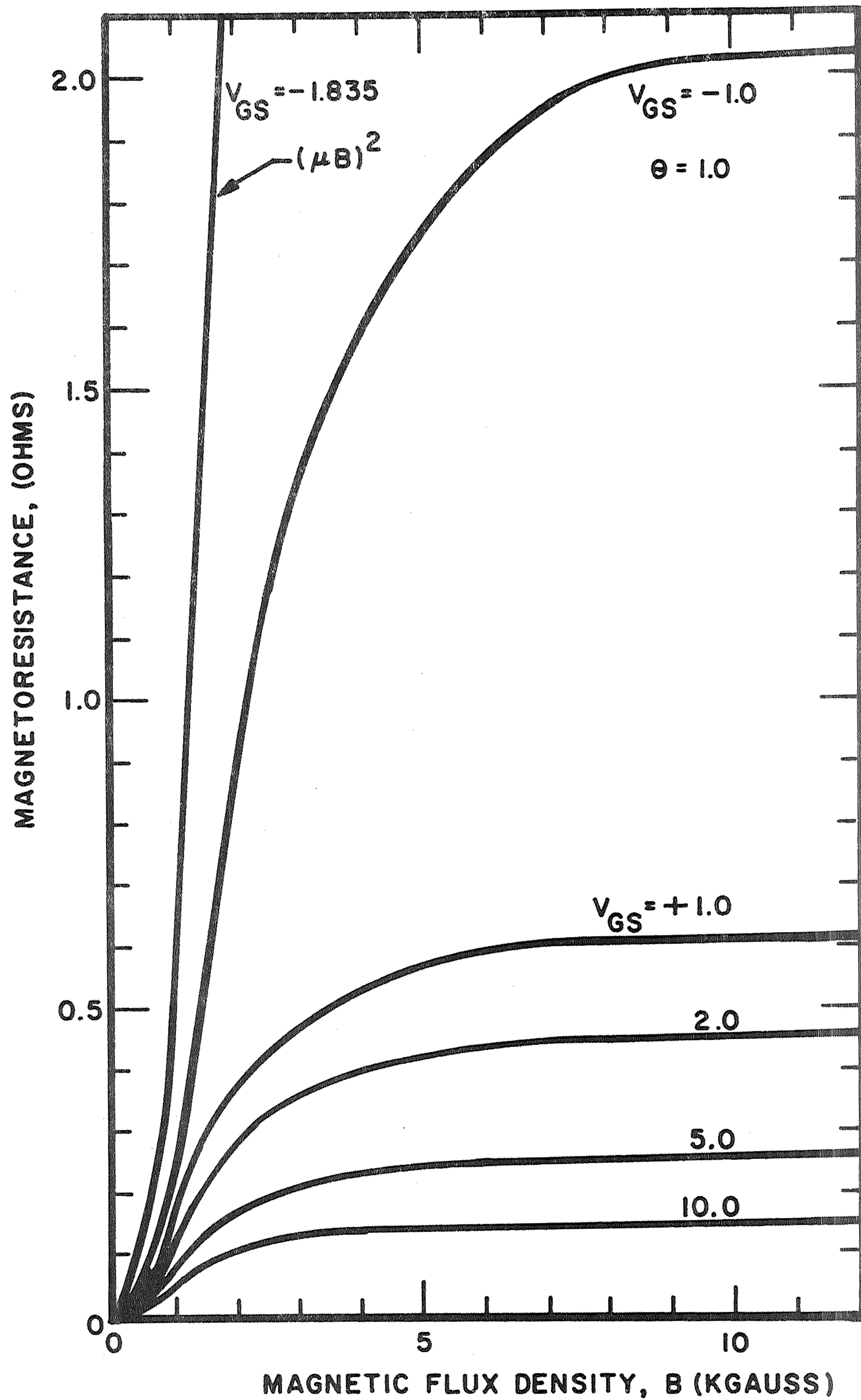

Figure 13. MIS corbino disk magnetoresistance vs. magnetic-flux density when θ = 1.0

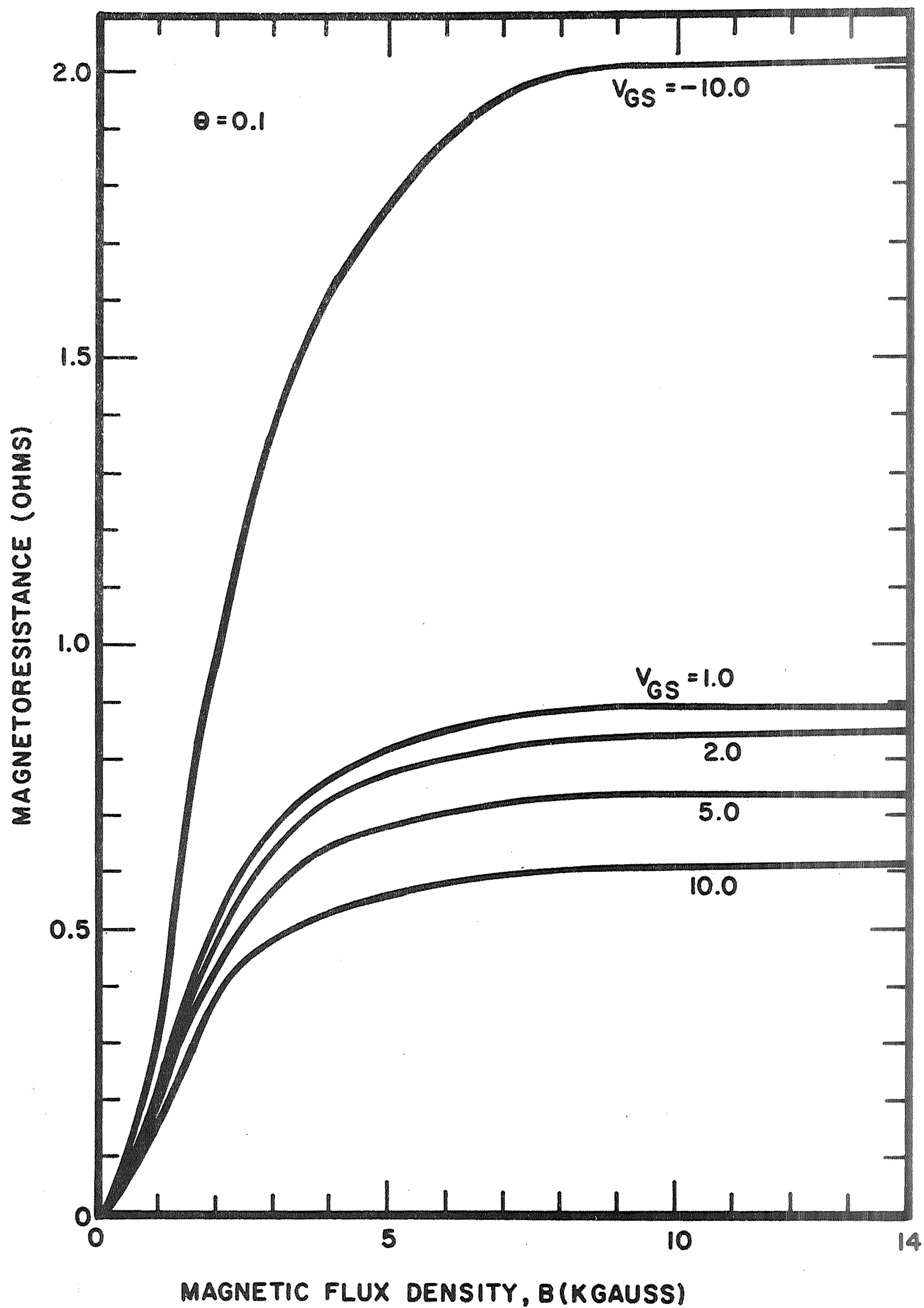

Figure 14. MIS corbino disk magnetoresistance vs. magnetic-flux density when θ = 0.1

B (Kgauss)	$V_{GS} = 10.0$ $MR = \frac{61B^2}{7.64+405B^2}$	$V_{GS} = -1.0$ $MR = \frac{61B^2}{1.469+28.6B^2}$	$V_{GS} = -1.835$ $MR = 61B^2$
0	0	0	0
0.5	0.0176	0.095	0.15
1	0.0522	0.348	0.61
2	0.1023	0.937	2.44
4	0.1347	1.610	9.75
6	0.1431	1.860	21.90
8	0.1463	2.000	39.60
10	0.1480	2.030	61.00

$\theta = 0.1$

B (Kgauss)	$V_{GS} = 1.0$ $MR = \frac{61B^2}{2.0861+66.3B^2}$	$V_{GS} = 2.0$ $MR = \frac{61B^2}{2.1523+70.4B^2}$	$V_{GS} = 5.0$ $MR = \frac{61B^2}{2.31+79.9B^2}$
0	0	0	0
0.5	0.0688	0.0658	0.0608
1	0.222	0.215	0.1960
2	0.516	0.495	0.4430
4	0.767	0.734	0.6460
6	0.843	0.805	0.7060
8	0.890	0.835	0.7310
10	0.893	0.850	0.7420

B (Kgauss)	$V_{GS} = 10.0$ $MR = \frac{61B^2}{2.591+97B^2}$	$V_{GS} = -10.0$ $MR = \frac{61B^2}{1.469+28.6B^2}$
0	0	0
0.5	0.0465	0.095
1	0.171	0.348
2	0.377	0.937
4	0.539	1.610
6	0.584	1.860
8	0.612	2.000
10	0.614	2.030

3.0 Electron Beam Source and Proposed Experimental Work

The CVC Vacuum System, CVI-18, is under modification. The electron beam source, Model TIH-270, Air Reduction

Company, Berkeley, California 94710, is installed in the vacuum chamber of the CVC system. The electron-beam-heated vapor source with 270° magnetic deflection requires a water-cooling system and a high voltage power supply with the controls.

3.1 Basic Principles

The electron beam source operates on principles not greatly different from those of a cathode-ray-tube. The cathode (filament) is operated at a negative high-voltage potential; the electrons are accelerated to the crucible which is at ground potential. The tungsten filament is heated to incandescence, causing electrons to be emitted in random directions. Thus, emission current is controlled by varying filament current. The filament is set in a cavity bounded by cathode blocks and a beam former, all at cathode potential. Space charges are formed by the emitted electrons at the back, bottom, and top of the cavity, forcing electrons emitted in these directions to return to the filament. Only electrons emitted at the front of the cavity escape. These are accelerated by the anode potential through a hole in the anode plate. During acceleration they are also focused, the plate operating somewhat as a single aperture lens. Beyond the anode plate, the electron beam is both deflected and further focused by a magnetic field onto a small spot on the evaporant metal in the crucible. The beam position controls vary the position of the electron beam on the crucible, and the dither controls allow the beam to be swept back and forth

longitudinally across the crucible. The sawtoogh dither waveform is superimposed on the quiescent DC beam position setting.

3.2 Specifications

Maximum accelerating voltage	10,000 V DC
Maximum gun power	10 KW (1 A at 10,000 V DC)
Minimum water flow at 25° C	1 gpm or 2 gpm for Al
Maximum water pressure	1000 psig
Focus coil voltage	18 V DC
Focus coil current	1.2 A normal, 3.0 A max.
Lateral sweep (dither)	
Voltage	28 V P.P. max.
Current	2.5 A max.
Filament number	202-3231 (0.031"ϕ, 6 turns)
Filament maximum	
Voltage	6 V AC
Current	28-35 A

The source is compatible with Airco Temescal Model ES-6A-210.

3.3 Advantages

The electron beam source and the electron-gun magnetic focusing system are shown in Figures 15 and 16. The electron-bombardment heated method has some significant advantages (Reference 10).

1. Upon impinging, most of the kinetic particle energy is converted into heat, and temperatures exceeding 3,000° C may be obtained.

2. Since the energy is imparted by charged particles, it can be concentrated on the evaporating surface while other

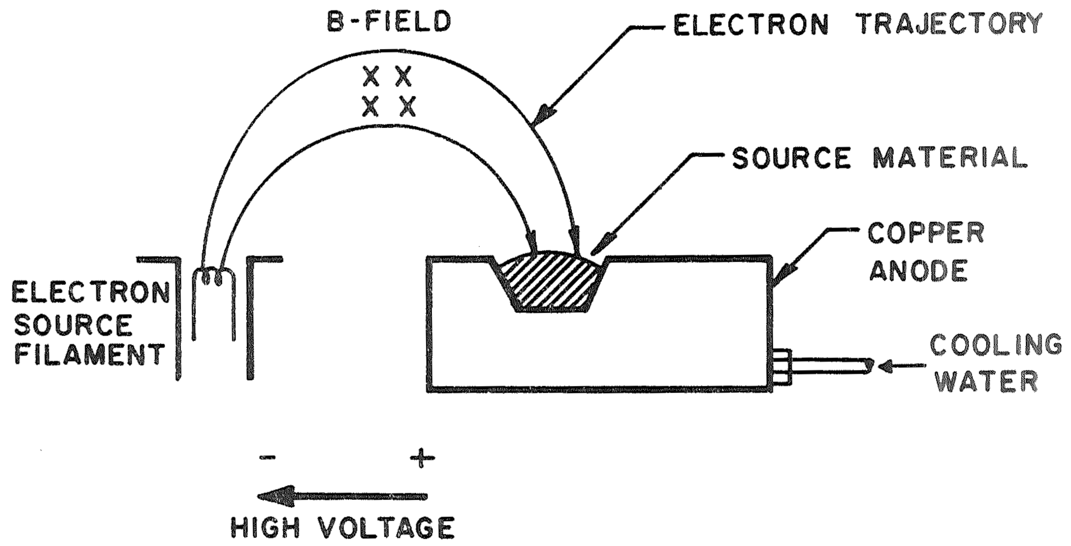

Figure 15. Electron beam source

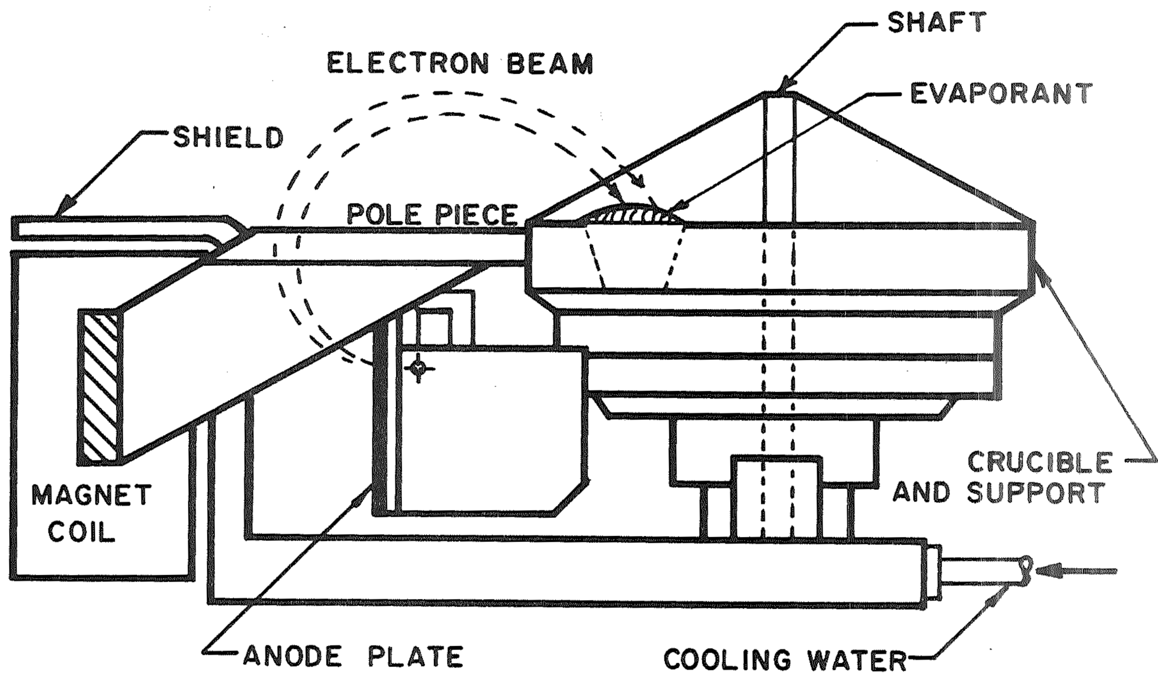

Figure 16. Electron Gun Focusing System

portions of the evaporant are maintained at lower temperatures. Hence, interaction between evaporant and support materials is greatly reduced.

3. Chemical reaction is negligible although the evaporant is in contact with the support surface. This is because a "skull" of solid evaporant is maintained at the interface and separates the melt from the support.

4. Electron beam heating sometimes offers other advantages such as greater simplicity of construction, more directional heat supply, or less stirring of the melt.

5. Electron-bombardment heating is used to evaporate compounds, provided these do not decompose upon heating. The heating is a very versatile and almost universal evaporation technique.

3.4 Proposed Experimental Work

In the previous sections, the expected results are obtained by calculation and plotted theoretically. Therefore, device fabrication and experiments are now needed.

It is very important in the experiment to study and anticipate the results so that if possible, curves (result) can be plotted before device fabrication and measurement. The plotted theoretical curves will be compared to the measured curves and analyzed thoroughly afterwards. If required, the device will be refabricated and measured according to the analyzed data. Through these processes, real and practical results are obtained.

The electron bombardment heating source is proposed to fabricate the high mobility thin films of the indium antimonide compound seniconductor because the source involves the capability of annealing the evaporated thin film. Furthermore, the insulator coating is possible using the source.

As soon as the installation of the beam source and the power supply is completed, fabrication of the InSb thin-film MIS devices will begin.

4.0 Conclusions

The data expected in the experimental work were obtained using the related equations. Actually, there are many factors to be considered in calculating the magnetoresistance; they are the mobility, conductivity, and geometry as well as the insulator thickness, gate-source voltage, ratio of effective drift mobility to true drift mobility, magnetic flux density, etc. As a result, the calculation involving the factors requires infinite time; therefore, the calculation is restricted to the possible limited values.

The electron-beam-heated vapor source (called electron gun) has many advantages so its installation in the vacuum chamber has been proposed and is in process. When the electron beam power supply, Model ES-6A-210 is repaired, device fabrication will start immediately.

In this report, practical results are not included because of the installation delay, but the calculated result will be used in the fabrication process and also be used for device analysis.

5.0 References

1. T. W. Kim, H. Y. Yu, and W. W. Grannemann, "Magnetoresistance Devices," Report No. PR-94(70), The University of New Mexico, March 1970.

2. T. W. Kim, H. Y. Yu, and W. W. Grannemann, "Metal-Insulator-Semiconductor (MIS) Magnetoresistance Devices Using the Thick Films of the InSb Compound Semiconductor Material," Report No. PR-96(70), The University of New Mexico, September 1970.

3. H. H. Wieder, Journal of Applied Physics, Vol. 40, No. 8, 1969, pp. 3320-3325.

4. A. C. Beer, "Galvanomagnetic Effects in Semiconductors," Solid State Physics Supplement 4, Academic Press, 1963, pp. 159-160.

5. A. C. Beer, Journal of Applied Physics, Vol. 32, 1961, p. 2107.

6. J. A. Carroll and J. F. Spivak, Solid-State Electronics, Vol. 9, Pergamon Press, 1966, pp. 383-387.

7. H. H. Wieder, Solid-State Communications, Vol. 3, 1965, pp. 159-160.

8. S. N. Levine, Micro- and Thin-Film Electronics Readings, Holt Rinehart Winston, 1964, pp. 317-324.

9. C. A. Simmons, "Influence of the Hall Mobility upon the Transverse Magnetoresistance in Indium Antimonide," Journal of Applied Physics, Vol. 32, No. 10, 1961, p. 1970.

10. L. I. Maissel and R. G. Lang, Handbook of Thin Film Technology, McGraw-Hill, 1970, pp. 1-50.